

Photomodulated thermoreflectance investigation at elevated temperatures: plasma versus thermal effect

Constantinos Christofides,^{a)} Andreas Othonos, and Efi Loizidou
Department of Physics, University of Cyprus, P.O. Box 20537, 1678 Nicosia, Cyprus

(Received 3 June 2002; accepted 6 December 2002)

Photomodulated thermoreflectance measurements were performed at elevated temperatures (294 to 623 K), on crystalline silicon lightly doped with boron. The temperature dependence is qualitatively and quantitatively discussed. The “competition” between thermal and plasma contribution, as a function of temperature, is one of the main subjects of this letter. © 2003 American Institute of Physics. [DOI: 10.1063/1.1541935]

In this letter, the characterization of lightly doped silicon samples at elevated temperatures is reported. As is well known, in typical PMTR experiments a light pulse from a pump laser source causes an increase in the local temperature of the sample, and this manifests itself as a change in the reflected probe beam. In general, the change in reflectivity is directly related to the heating of the lattice by the pump beam; this heating affects the temperature dependence of the material’s optical constant. In the case of semiconductors, however, there is an additional effect: the creation of electron–hole pairs. In general, we can write the total induced photomodulated contribution as a sum of the thermal and plasma contribution:^{1–5}

$$\frac{\Delta R}{R_0} = \frac{1}{R_0} \left(\frac{\partial R}{\partial T} \right) \Delta T + \frac{1}{R_0} \left(\frac{\partial R}{\partial N} \right) \Delta N, \quad (1)$$

where R_0 is the reflectivity at temperature T_0 and plasma density N_0 . The first term on the right side is the temperature coefficient of reflectivity and the second term is the plasma coefficient of reflectivity, which can also be negative. ΔR , ΔT , and ΔN are the local variations of the reflectance, temperature, and plasma density, respectively, induced by the absorption of the laser pump beam. Thus, we can express the total PMTR signal $\Delta R/R_0$, as

$$\frac{\Delta R}{R_0} = \frac{\Delta R_{\text{th}}}{R_0} + \frac{\Delta R_{\text{pl}}}{R_0}, \quad (2)$$

where ΔR_{th} and ΔR_{pl} are the photothermal signal components due to the thermal and plasma effects, respectively. It has been shown that the photothermal signal will be proportional to the variations in the surface temperature. The resulting signal amplitude attributed to the thermal contribution may be written as³

$$\frac{\Delta R_{\text{th}}(T)}{R_0} \approx \frac{H}{\sqrt{\omega \rho C \kappa(T)}} \quad (3)$$

where ρ is the density of the solid, C the specific heat at constant volume, and κ is the thermal conductivity, which depends strongly on temperature. The essentially temperature-independent factor H is a function of the real and imaginary parts of the medium refractive index and the local temperature derivatives of real and imaginary parts of

the dielectric constant. We note that the signal is inversely proportional to the square root of angular frequency, $\omega = 2\pi f$ (where f is the modulation frequency). It is also inversely proportional to the sample thermal conductivity κ , which is a function of lattice temperature.

The effect of the photogenerated plasma becomes important for $\omega\tau \geq 1$, which was also studied by several workers.^{1–5} Assuming spatially homogeneous e–h plasma, and a simple Drude effect model, the plasma reflectance is expressed by

$$\frac{\Delta R_{\text{pl}}(T)}{R_0} \approx - \frac{2\lambda^2 e^2}{\pi m^* v_c^2} \frac{\Delta N}{n(n^2 - 1)}, \quad (4)$$

where e is the electron charge, m^* is the electron’s effective mass, v_c is the velocity of the light, and λ is the optical wavelength of the probe laser. The temperature-varying parameters in the above expression are the real part of the refractive index n , and the excess plasma density ΔN . As a result, the term $[n(n^2 - 1)]^{-1}$ varies less than 2% between 294 and 623 K.⁶

It is well known that in the case of low modulation frequency ($\omega\tau \ll 1$), the PMTR signal is dominated by the thermal contribution. On the other hand, at higher frequencies ($\omega\tau \geq 1$), we have a competition between thermal and plasma effects. In this letter, we present the extension of the conventional laser-induced, photomodulated, thermoreflectance method for measurements at elevated temperatures. The experimental configuration is similar to the one employed in the past,^{1–4} with the important addition of the temperature sensing-controlling equipment. The sample is placed in the high-temperature chamber. The sample holder is isolated by a ceramic element in order to limit the heat diffusion to the surrounding area. The chamber was equipped with suitable incoming and exhaust nitrogen gas. A gas flow through the chamber during the high-temperature photothermal measurements avoided any oxidation of the semiconducting surface. On the cell, optical access is also available through a quartz window. The periodic sample heating was obtained with Ar⁺ laser beam (488 nm), modulated by an acousto-optic modulator. This beam, with incident power of approximately 100 mW, was focused normally onto a sample surface to a spot size of about 40 μm . The changes in the reflectivity of the He–Ne laser beam (632.8 nm) were measured by a silicon photodiode. PMTR measurements were taken in the temperature range between 294 and 623 K and at

^{a)}Electronic mail: costasc@ucy.ac.cy

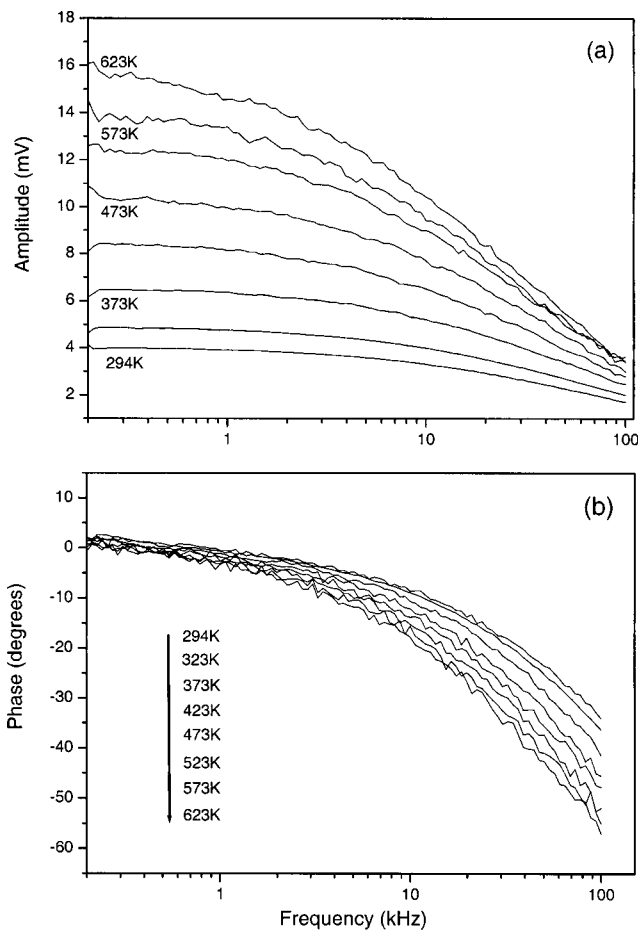


FIG. 1. PMTR signal versus modulation frequency for the lightly doped, crystalline silicon sample at various temperatures in the range of 294 to 623 K: (a) PMTR amplitude signal and (b) PMTR phase signal.

modulation frequencies between 100 Hz and 100 kHz using a lock-in amplifier. After the stabilization of the temperature, the amplitude and phase signal were stored in a computer. The sample used in these experiments was crystalline silicon wafer lightly doped with boron ($\rho \approx 20\text{--}25 \Omega \text{ cm}$).

The PMTR signal is simply the change in modulated reflectance ΔR , and not the normalized reflectance signal $\Delta R/R_0$ (R_0 is the dc reflectivity). In fact, the dc reflectivity varies little with lattice temperature. In the range of our measurements at $\lambda = 632.8 \text{ nm}$ (He-Ne), the variation of R_0 is less than 5%. At 294 K $R_0 = 37\%$, while at 623 K the dc reflectivity becomes $R_0 = 38.8\%$.^{6,7} This theoretical result was verified experimentally. The reflectivity measurements (using only the probe He-Ne beam) were performed throughout the temperature range 294 to 623 K, and the signal was essentially constant. Taking into account these results, the changes of the background reflectivity R_0 have been ignored in the rest of this work. In addition, the linearity of the PMTR signal versus temperature was verified.

Figure 1(a) shows the variation of the PMTR signal amplitude versus modulation frequency for the lightly doped crystalline silicon sample, at various temperatures in the range of 294 to 624 K. Figure 1(b) shows the variation of the PMTR phase for the same sample. As expected, with respect to the frequency we can point out the decrease of the PMTR signal with increasing modulation frequency. The dependence of the PMTR signal on frequency is obvious and is in

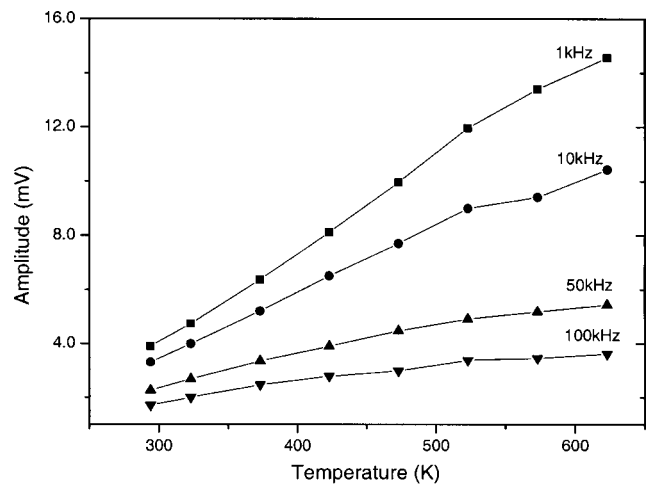


FIG. 2. PMTR signal amplitude versus temperature for the lightly doped, crystalline silicon sample at four different modulation frequencies: 1, 10, 50, and 100 kHz.

agreement with several simulation and experimental results presented in the past.^{1-5,8} At room temperature (294 K), we note that the phase varies from 0° to -35° in the frequency range between 100 Hz and 100 kHz. This phase shift is in agreement with several theoretical simulations performed in the literature.⁹ On the other hand, one can see that at elevated temperatures, the phase shift increase becomes more significant. This phenomenon is more pronounced at higher frequencies. In Fig. 2(a), we present the PMTR experimental data versus temperature at the various modulation frequencies: 1, 10, 50, and 100 kHz. We note the decrease of the PMTR signal with increasing frequency.

One of the main objectives of this letter is to examine and discuss the variation of the signal versus temperature. As is well known for low frequencies, such as 1 kHz, the signal is completely due to the thermal effect and can be fitted by Eq. (3). On the other hand, at 100 kHz, the PMTR signal is induced from a thermal as well as from plasma component. In Figs. 3(a) and 3(b), we present the experimental data taken from Fig. 2, as well as some theoretical fittings. First, we try to fit the “thermal” experimental data using Eq. (3) [dotted line, Fig. 3(a)]. It is obvious that this fitting is not in agreement with the experimental data. The temperature change of the thermal conductivity cannot justify completely the variation of the PMTR signal since it decreases by half between 294 to 650 K.¹⁰ In fact, in order to better adjust to the theory, one must take into account the change of the absorption coefficient α of the doped silicon versus temperature. We note that α varies from 5×10^3 to $1.1 \times 10^4 \text{ cm}^{-1}$, thereby increasing the amount of light energy absorbed at the surface, and consequently the PMTR signal.⁶ Thus, one can rewrite Eq. (1) by taking into account the variation of the optical absorption coefficient $\alpha(T)$:

$$\frac{\Delta R_{th}(T)}{R_0} \approx \frac{H}{\sqrt{\omega \rho C \kappa(T)}} \frac{\alpha(T)}{\alpha(294)} \quad (5)$$

The dashed line in Fig. 3(a) presents the new theoretical fitting, taking into account the correction introduced in Eq. (5). We see that a better fitting is achieved for the PMTR data. Finally, the solid line presents the theoretical fitting

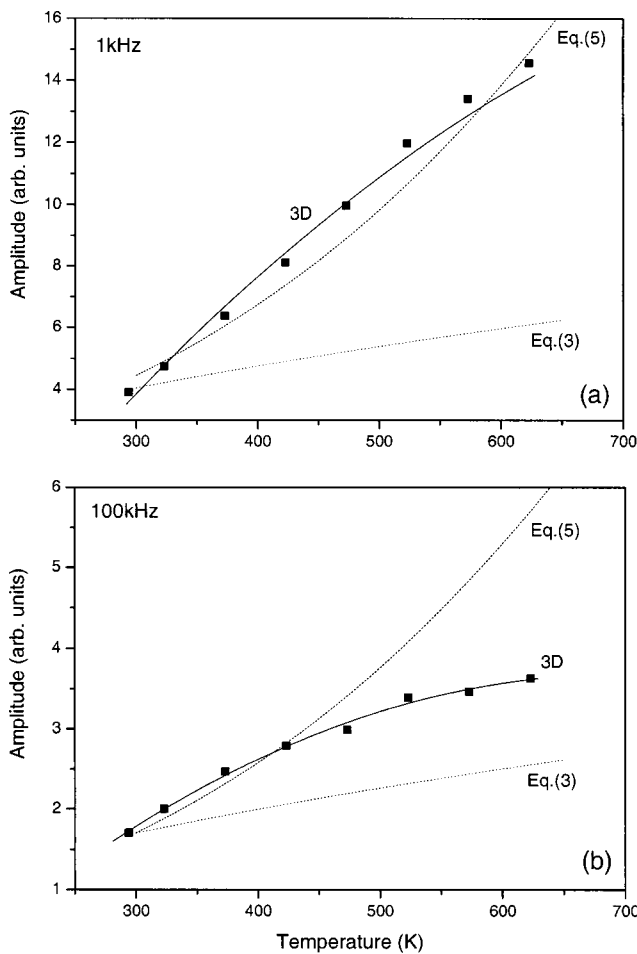


FIG. 3. PMTR signal amplitude versus temperature for the lightly doped, crystalline silicon sample at two different modulation frequencies: (a) 1 KHz and (b) 100 kHz. The dotted line presents Eq. (3), the dashed line presents Eq. (5) and the symbol ■ represents the experimental points.

obtained from the photothermal three-dimensional (3D) solution as was presented in detail in the past.⁵ It is important to note that a very precise analysis has been performed in order to check if the 3D solution can be applied at elevated temperature, where the thermal activation term may not be negligible. This analysis has already been published elsewhere and confirms our experimental and theoretical findings.¹¹

In Fig. 3(b), we present the experimental data obtained from Fig. 2(b) for a modulation frequency of 100 kHz. The dotted line presents the estimated PMTR signal using Eq. (3). As in Fig. 3(a), Eq. (3) cannot fit to the experimental data, because (a) one has to take into account the variation of the absorption coefficient versus temperature and (b) at high frequency, one must also take into account the plasma contribution of Eq. (4) that is present at high frequencies, such as 100 kHz. The dashed line of Fig. 3(b) presents the theoretical fitting of Eq. (5) (which includes the optical absorption correction). We note that the discrepancy is still present and is even more pronounced at higher temperatures, where the lifetime τ is longer (between 294 and 623 K the lifetime varies between 7.7×10^{-4} s and 12×10^{-4} s). Thus, for a constant frequency at a temperature of 623 K the product $\omega\tau$

is greater than at 294 K. As it was mentioned previously, the plasma contribution will be noticeable only when the values of the product $\omega\tau$ are close to or greater than unity. This product depends on the working experimental temperature, since the relaxation time increases with temperature in the range of 294 to 623 K. This explains why at higher temperatures the discrepancy is larger. Contrary to the case of 1 kHz, the theoretical fitting [using Eq. (5)] overestimates the experimental data. This was expected, because for high frequencies the PMTR is induced not only from the thermal but also from the plasma component. The dashed line of Fig. 3(b) includes only the thermal contribution. By adding to the dashed line the plasma contribution, *which is negative*, it is obvious that we will better approach the experimental points. It is of course more complicated to estimate quantitatively the plasma term of Eq. (4). In fact, as it was pointed out earlier, the temperature variation of the term $[n(n^2-1)]^{-1}$ is insignificant and its influence on the PMTR signal is negligible. This small change cannot justify the difference between experimental data and theory. The temperature dependence of the ΔN term is more difficult to quantify because of the ambipolar diffusion coefficient complex temperature dependence. The solid line in Fig. 3(b) is obtained by using the 3D theoretical model obtained in the past.⁵ We note that in this case an excellent agreement can be reached.

In conclusion, one can point out the strong dependence of the PMTR signal on the lattice temperature. This dependence has been explained in terms of the variation of the thermal and plasma wave contributions. The influence of various physical parameters, such as thermal conductivity, optical absorption coefficient, and carrier lifetime, has been examined. The use of the PMTR technique at elevated temperatures, for the characterization of semiconducting materials, has been proven to be a useful technique in semiconductor technology. PMTR can be developed as an excellent tool for real-time measurements during the growth, annealing, and deposition of semiconducting films, even at high temperatures.

The support of the Research Promotion Foundation of the Government of Cyprus under the “IIENEK 14/2000” is gratefully acknowledged.

¹ A. Rosencwaig, J. Opsal, W. L. Smith, and D. L. Willenborg, Appl. Phys. Lett. **46**, 1013 (1985).

² J. Opsal, M. W. Taylor, W. L. Smith, and A. Rosencwaig, J. Appl. Phys. **61**, 240 (1986).

³ I. A. Vitkin, C. Christofides, and A. Mandelis, Appl. Phys. Lett. **54**, 2392 (1989).

⁴ I. A. Vitkin, C. Christofides, and A. Mandelis, J. Appl. Phys. **67**, 2822 (1990).

⁵ M. Nestoros, B. C. Forget, C. Christofides, and A. Seas, Phys. Rev. B **51**, 14115 (1995).

⁶ T. Tomita, T. Kinosada, T. Yamashita, M. Shiota, and T. Sakurai, Jpn. J. Appl. Phys. **25**, L925 (1986).

⁷ S. M. Sze, *Physics of Semiconductor Devices* (Wiley-Interscience, London, 1969), Chap. 2.

⁸ A. Seas and C. Christofides, Appl. Phys. Lett. **66**, 3346 (1995).

⁹ B. C. Forget, Ph.D. Thesis, Université de Paris VI, 1993.

¹⁰ J. R. Meyer, M. R. Kruer, and F. J. Bartoli, J. Appl. Phys. **51**, 5513 (1980).

¹¹ C. Christofides, A. Othonos, and E. Loizidou, J. Appl. Phys. **92**, 1280 (2002).